



This is a repository copy of *Ultrasonic Imaging of the Piston Ring Oil Film during operation in a Motored Engine – Towards Oil Film Measurement*.

White Rose Research Online URL for this paper:
<http://eprints.whiterose.ac.uk/86932/>

Version: Accepted Version

Article:

Avan, E.Y., Mills, R.S. and Dwyer-Joyce, R.S. (2010) Ultrasonic Imaging of the Piston Ring Oil Film during operation in a Motored Engine – Towards Oil Film Measurement. SAE International Journal of Fuels and Lubricants, 3. 786 - 793.

<https://doi.org/10.4271/2010-01-2179>

Reuse

Unless indicated otherwise, fulltext items are protected by copyright with all rights reserved. The copyright exception in section 29 of the Copyright, Designs and Patents Act 1988 allows the making of a single copy solely for the purpose of non-commercial research or private study within the limits of fair dealing. The publisher or other rights-holder may allow further reproduction and re-use of this version - refer to the White Rose Research Online record for this item. Where records identify the publisher as the copyright holder, users can verify any specific terms of use on the publisher's website.

Takedown

If you consider content in White Rose Research Online to be in breach of UK law, please notify us by emailing eprints@whiterose.ac.uk including the URL of the record and the reason for the withdrawal request.



eprints@whiterose.ac.uk
<https://eprints.whiterose.ac.uk/>

Ultrasonic Imaging of the Piston Ring Oil Film During Operation in a Motored Engine - Towards Oil Film Thickness Measurement

Author, co-author (Do NOT enter this information. It will be pulled from participant tab in MyTechZone)

Affiliation (Do NOT enter this information. It will be pulled from participant tab in MyTechZone)

Copyright © 2011 SAE International

ABSTRACT

The oil film that forms between piston rings and cylinder liners is an essential parameter which influences parasitic loss and emission rates in an internal combustion (IC) engine. Several methods have been used to analyse these thin oil films in the past, however, all these methods have required invasive access to the contact area via a window or a surface mounted sensor in the cylinder wall or liner. This paper introduces a novel approach for the imaging of the piston ring – cylinder contact, non-invasively.

A straight beam ultrasonic contact transducer was coupled to the wet-side of the cylinder wall of a motored diesel engine. Ultrasonic waves were propagated through the cylinder wall and reflections from the ring-liner contact were recorded as the piston rings passed over the sensing area. The proportion of an ultrasonic pulse that is reflected from the layer, known as reflection coefficient, varies with the stiffness of the layer and the acoustic properties of the matching materials and lubricant. The transducer has successfully detected the rings and the reflection coefficient has been generated using the recorded reflection from the contact. Future evaluation of the oil film thickness (OFT) at the ring contact has been proposed using various ultrasonic transducers.

INTRODUCTION

Power loss in the ring-liner contact is one of the most critical issues in an internal combustion engine affecting operation and efficiency. The formation of an oil film in this contact is an essential parameter for analyzing oil availability and its distribution over the contact area. Proper control of the film allows; a decrease in fuel and oil consumption, reduction in ring and liner wear, increase in engine power output and a reduction in harmful exhaust emission.

Several methods have been applied to enable ring-liner film thickness measurements. Capacitance [1-4] and laser induced fluorescence (LIF) techniques [5-7] have successfully been applied for piston ring lubrication. However, both of these methods require the need to penetrate the cylinder wall or liner in order to access the piston ring-wall contact area. Table 1 shows OFT range and methods in selected literature.

Table 1 – Measured ring film thicknesses in literature.

*(Eddy C.: Eddy Current, Cap: Capacitance, F:Fired, M:Motored) * Approximate range deduced from the graphs*

Ref. Num.	Method	Engine	OFT range (µm)	Engine Speed (rpm)
[10]	Eddy C.	F	1.0 – 19	900
[6]	LIF	F	0.4 – 4.0	1500–2000
[7]	LIF	F	1.0 – 4.5	1000
[8]	LIF	F	0.6 – 3.5	2000
[9]	LIF	M	*5.0 – 18	300-1200
[1]	Cap.	F	1.0 – 10	1000-1900
[2]	Cap.	F	4.0 – 23	2000
[4]	Cap.	M	0.2 – 8.0	1300-1400

In this paper, we explore the process of imaging the piston rings using reflected ultrasound and then show how oil film thickness measurements can be made using this reflection data. This approach involves continually passing pulses of ultrasound through the cylinder wall. When no ring is present, the ultrasonic pulse will be completely reflected, but when there is a ring present, some of the ultrasound is transmitted through the interface into the ring. This method is non-invasive and does not require penetration of the cylinder wall. However high speed ultrasound pulsing and data acquisition is required to capture the passage of the rings.

The proportion of the incident wave amplitude that is reflected is expressed by the reflection coefficient using,

$$R = \frac{A_r}{A_i} \quad (1)$$

where A_i is the incident wave amplitude and A_r is the reflected wave amplitude. Figure 1 shows five cases; (a) an ideal interface between two identical materials, (b) an ideal interface between two dissimilar materials, (c) an interface between a solid and air, (d) an interface between dissimilar materials with an intermediate layer, (e) an interface between a solid and air, with a thin layer of oil on the surface.

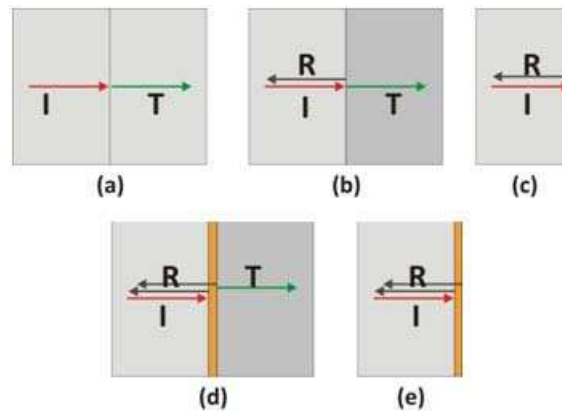


Figure 1. Reflections from ideal interface configurations

For case (a) the incident wave is completely transmitted to the matching material and $R=0$, if the matching materials are different, which is depicted in case (b), then the proportion that is reflected from the interface is given by;

$$R = \frac{z_1 - z_2}{z_1 + z_2} \quad (2)$$

where, z , is the acoustic impedance of the interface materials and the subscripts denote the position of the materials either side of the interface. It is difficult measure the incident signal, but if the matching material is air, case(c), most of the incident wave is reflected due to a high acoustic mismatch between the materials. Hence, in practice, the incident signal can be recorded using this reflection. However, if the incident wave strikes a layer rather than an interface, case (d), then the wave is reflected back from the front and back face of the layer. If the layer is very thin then the two reflections are close together. This situation can be modeled by using a quasi-static spring model. Tattersall [11] demonstrated that the reflection coefficient for a thin layer is defined by,

$$R = \frac{(z_1 - z_2) + i\omega / K(z_1 z_2)}{(z_1 + z_2) + i\omega / K(z_1 z_2)} \quad (3)$$

where, ω , is the angular frequency of the ultrasonic wave ($2\pi f$) and, K , is the stiffness of the interfacial layer. For the same reason as described in case (c), the incident signal for the layer can be recorded using the reflection in case (e).

TEST APPARATUS

THE MOTORED ENGINE

A Perkins Engine 1100 Series was modified to be driven by an external electric motor. The engine's valve train and head were removed. The lubricant and water systems were modified to lubricate and cool just the cylinder block. There are a number of access points on the engine to mount the transducer on the outside surface of the cylinder walls. The block, made from cast iron, had 4 cylinders with a displacement of 4.4litres, a bore of 105mm and a stroke of 127mm. A shaft encoder was connected to the crankshaft in order to gain a feedback of both engine speed and timing pulse for triggering the transducer. The oil used in the measurement was 15W-40 multi grade oil.

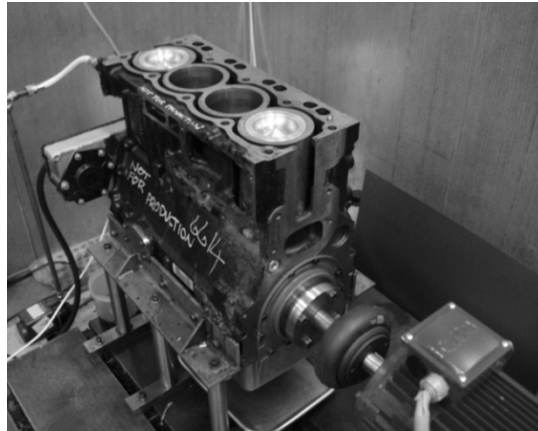


Figure 2. Motored Engine used in the tests

ULTRASOUND INSTRUMENTATION

The ultrasonic equipment consisted of an ultrasonic pulser-receiver (UPR), a 5 MHz straight beam ultrasonic contact transducer, an oscilloscope and a dedicated PC. A schematic view of the test equipment and their connections is shown in Figure 3. A LeCroy LT342 oscilloscope was used in this study, which allowed signal voltages to be viewed additionally to be digitized before downloading the data into the PC for signal processing. The scope samples at a bandwidth of 500 MHz and the sampling rate is 500 Msamples/second. It has 250 kB internal memory capacity.

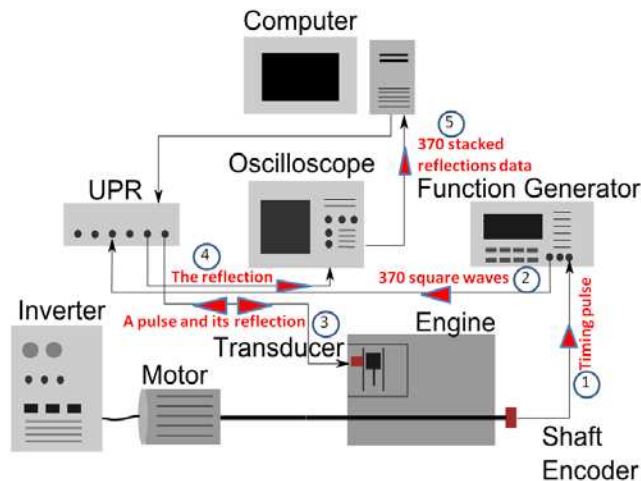


Figure 3. Schematic diagram of the test equipments and their connections

The 5MHz contact transducer, shown in Figure 4, was coupled to the wet-side of the cylinder wall using a magnetic clamp. Liquid coupling was applied on the interface between the transducer and outside surface of the cylinder wall to prevent air going into the interface. This liquid coupling allows transmitting of ultrasound from the transducer to the medium due to higher acoustic impedance and lower attenuation compared with air.

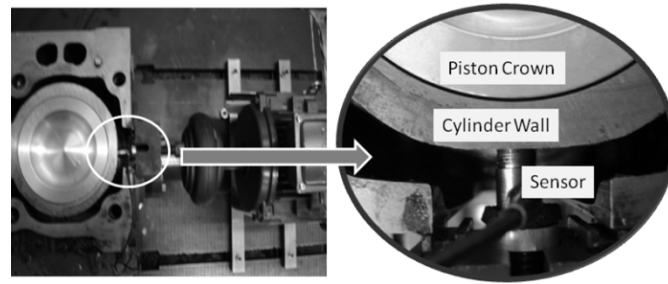


Figure 4. A top view of the engine showing the transducer location

TEST PROCEDURE

The contact transducer was coupled to the wet-side of the cylinder wall of the motored diesel engine. The ultrasonic reflection measurements start with a timing pulse from the shaft encoder (see Figure 3). The timing of this pulse can be adjusted according to the desired piston position inside the cylinder (e.g. TDC), which is namely called the triggering point. When the piston is on the triggering point, the shaft encoder sends the timing pulse to the function generator, which generates a defined number of square waves (e.g. 370 square waves). These square waves are used as an external triggering source for the UPR, which produces and sends an equivalent number of short duration high voltage signals to the transducer. A piezo element inside the transducer is excited by these voltage signals and generates ultrasound waves which propagate through the cylinder wall. The transducer operates in a pulse-echo mode, therefore, it captures the reflections from the cylinder as the piston rings pass over the transducer area. These reflected signals are amplified and sent through the oscilloscope. The pulse of interest (b in Figure 5) is selected for each of the reflected signals. These selected segments (they constitute a pulse sequence) are digitised and stored by the oscilloscope and then the data is downloaded to the computer.

SIGNAL PROCESSING

Once the data is passed to the computer, the reference signal is created by averaging the initial reflections in the pulse sequence because the triggering system allows a reflected signal to be recorded at a time before the rings reach the transducer location. Hence, initial reflections in the pulse sequence are from the reference interface (case (e) in Figure 1) and the remainder from the layer (ring-oil-wall, case(d) in Figure 1). A fast Fourier transform (FFT) is performed on both the reference signal and each reflected signal, giving the amplitude variation in the frequency domain. The next step is to calculate the reflection coefficient, which is obtained by dividing the FFT of reflected signal by the FFT of reference signal.

In the experimental stage, the average of the FFT's for the first 5 pulses in the pulse sequence were used to generate the reference signal. TDC, BDC and the middle section of the cylinder (MID) were separately used to specify when the system should be triggered. A square wave with 370 cycles was produced by the function generator for each shaft encoder timing pulse. The number of cycles was determined by the storage limitation of the oscilloscope. To obtain an optimum number of data points, the scope was set to acquire 370 segments of which each contained 500 sample points sampled at 500 MS/s (2 ns/pt). The frequency of the triggering square waves was selected according to the piston speed to ensure that the entire ring pack was captured.

RESULTS

Figure 5 shows a sample time domain plot of the reflected signal from the cylinder wall. The peak (a) is a combination of sensor initiation and reflection from the wet-side of the cylinder, while the peak (b) is the reflection from the inner cylinder wall and is changing as the piston rings pass over the transducer location.

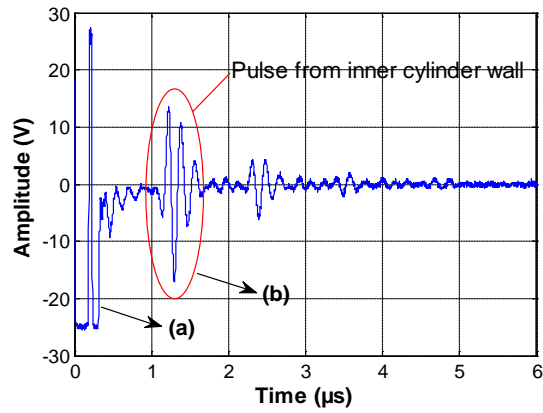


Figure 5. Time domain signal showing the reflections from the cylinder wall

Figure 6 shows samples of a reference signal and a reflected signal captured when an oil film was formed between the piston ring and wall. As mentioned above, the reference signal was recorded from the reference interface. If the FFT is applied to these samples, the frequency domain pulses, in Figure 7, are obtained. It is seen that the amplitude of the pulse is decreasing when oil formed in piston ring.

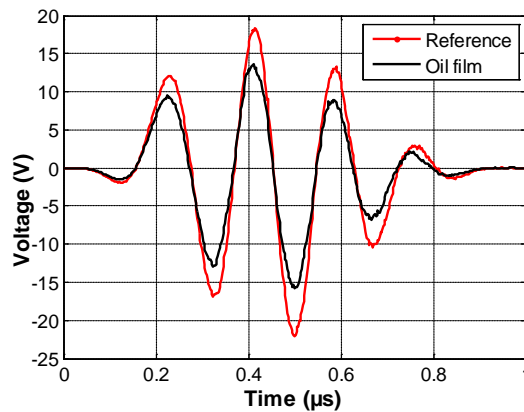


Figure 6. Time domain signals showing the variation of the marked peak (b) the as a piston ring is passing over the sensing area

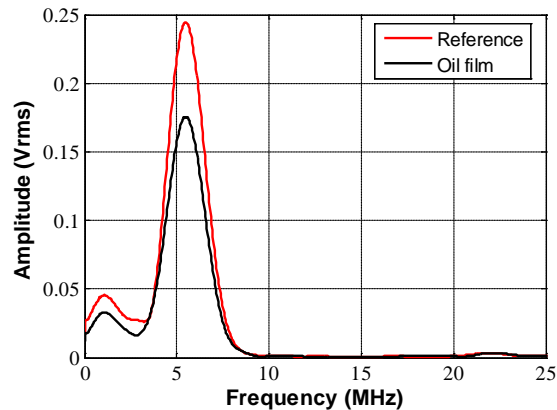


Figure 7. Frequency domain signals showing the variation of the marked peak (b) as an oil film formed between piston ring and cylinder wall

The reflection coefficient was produced by dividing the FFT amplitude of the reflected signals by the FFT amplitude of the reference signal. Figure 8 shows the reflection coefficient when the engine speed was 840 rpm. The data was captured when the piston was travelling from TDC to BDC. The three troughs associated with the three rings can be seen clearly in the figure. The first trough

corresponds to the passage of oil ring and the second and the third troughs represent the passage of second ring and the top ring respectively.

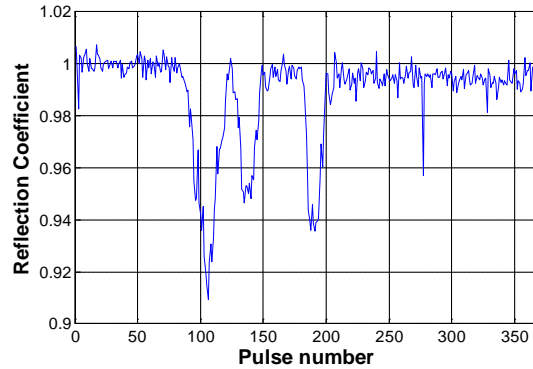


Figure 8. Plot of reflection coefficient for an engine speed of 840 rpm.

When the piston ring is far from the transducer's inspection area, the reflection coefficient approaches unity because all the ultrasonic waves are reflected back from the interface. As the piston rings pass through the area, the reflection coefficient becomes less than unity. However, in the figure, there are small spikes and noise which could either be electrical interference or the thin layer of oil on the inside cylinder wall which is inhomogeneous and causes some reduction in reflection.

Figure 8 shows the data in terms of pulse number. Pulses are triggered by the function generator; total time for pulsing can be calculated from time interval between the pulses (i.e. an inverse of pulse frequency) multiplied by the number of pulses, thus it gives the time sequence. To find out an angular displacement of crankshaft during this pulsing time, the motor frequency is then multiplied by the time sequence. The piston displacement can be obtained after basic trigonometric calculations in which required parameters are only piston rod length, angular displacement and diameter of crank shaft.

The ultrasonic reflection measurements were taken from three locations which were close to TDC, BDC and MID of the motored engine as the piston was moving down for the three engine speeds 600, 720, 840 rpm. Figure 9 shows the minimum reflection coefficients of the piston ring-wall contact at these locations. The reflection coefficients were varying between 0.88 and 0.97. The smallest R values were measured at close to BDC.

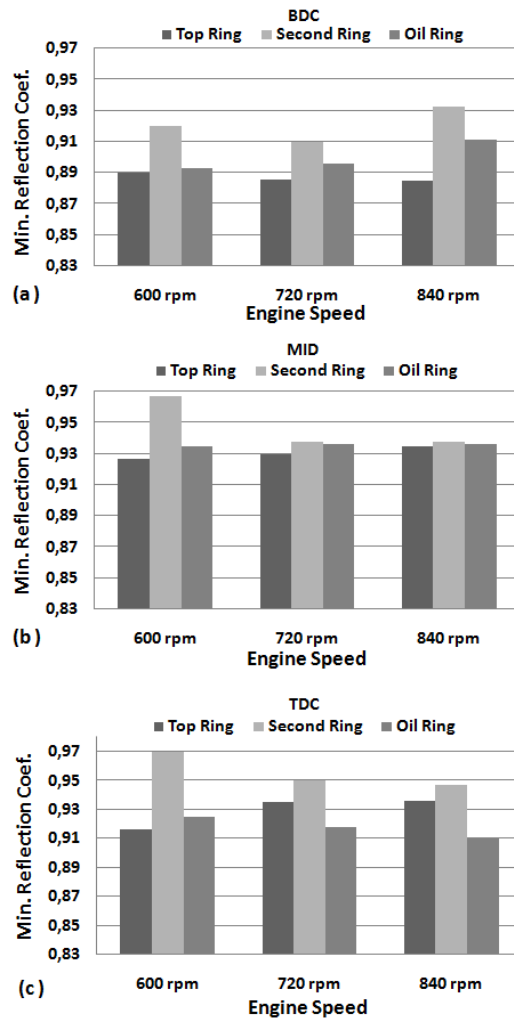


Figure 9. Graphs (a,b and c) of minimum reflection coefficients for the rings with various engine speeds.

DISCUSSION

SAMPLING RATE AND DATA CAPTURE

Segment numbers, which constitute the pulse sequence, have an effect on the accuracy of the measurement because they are successive the pulse of interest signals in which some of the signals are reflections from the ring. If more segments for the rings are used, more accurate data can be obtained. However, each of the signals in the pulse sequence is digitized at a selected sampling rate and utilizes the internal memory capacity. For example, if a signal with duration of $2 \mu\text{s}$ is digitized at 25 MS/s , it is defined by 50 data points while this signal is represented by 500 data points for 250 MS/s digitizing. The internal memory capacity of the scope is 250 kB. This capacity is used to store the data in real time for transmitting to the dedicated PC. In the experiments, 370 segmented signals were digitized at 500 MS/s . An increase in data storage capacity of the system would allow more data points per signals and more segmented signals to be captured.

TEMPERATURE AND SENSOR'S THERMAL SENSITIVITY

Certain ultrasonic sensors can be used to capture reflections in high temperature applications. Dwyer-Joyce et al. investigated the skirt-liner film in both motored and fired engine configuration using a piezo-electric element [12]. The increase in temperature can have an effect on the response of the ultrasonic transducer. However, continual updating of the reference measurement (i.e. cycle by cycle), was performed by averaging the first five pulses in the pulse sequence, at which time no piston rings were present. Hence the

reference and measurement signals have been taken at the same temperature, meaning that every pulse sequence has its own reference pulse. This provides automatic response calibration for the transducer.

SPATIAL RESOLUTION

The transducer used in the tests has successfully detected all the rings but its piezo element diameter is bigger than the ring width and Figure 10 schematically shows the effect of this. The ultrasound pulse is emitted over a larger area than the piston ring contact. This means that some of the pulse is reflected from the oil film and some from the wall-air boundary (albeit with a thin oil layer present on the surface). The reflected signal is thus a combination of cases (d) and (e) in Figure 1. Therefore the reflection coefficient is a combination of equations 2 and 3.

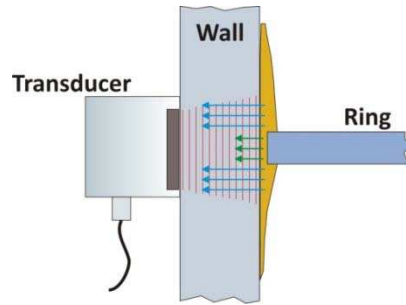


Figure 10. Reflections from both ring and wall-air boundary captured by the piezo element

To use a transducer with a diameter of at least equal to the ring width or smaller would be useful. On the other hand, more powerful ultrasonic beam can be focused down to a point, considerably smaller than the ring width. An immersion type transducer has a capability of such a focusing function. Additionally, to reduce the ring edge effect on measurements, a transducer with a higher centre of frequency could be chosen, such as 25 MHz or 50 MHz. The use of high frequency transducer also provides better signal resolution over small area; however optimum choice should be made considering the increase in attenuation rate of ultrasound with high frequency.

TOWARDS OIL FILM MEASUREMENT

If the incident ultrasound can be confined to fall entirely on the ring surface then equation 3 can be applied. This relates the reflection coefficient to the stiffness of the interfacial layer, K . This is the key to measuring oil film thickness because this stiffness is related to the film thickness by the relationship;

$$K = \frac{B}{h} \quad (4)$$

where B , is the bulk modulus and h , is the thickness of the layer. Thus a thin layer is very stiff and would allow most of the sound wave to be transmitted. Equation (4) can be rewritten in terms of the acoustic properties of the layer material by substituting, $c^2 = B/\rho$, where c is the speed of sound in the layer and ρ is its density. This gives,

$$K = \frac{\rho c^2}{h} \quad (5)$$

This stiffness can be used in the quasi-static spring model for identical materials either side of the interface ($z_1 = z_2$) and so equation (3) becomes:

$$h = \frac{\rho c^2}{\pi f z} \sqrt{\frac{|R|^2}{1 - |R|^2}} \quad (6)$$

This relationship gives the layer thickness in terms of reflection coefficient and acoustic properties of the oil and materials either side of the interface [10].

References [12-16] show where this method has been used to quantify oil film thickness. There are several approaches to achieving this for the piston ring case. Firstly, it would be ideal to use a transducer smaller than the piston ring width. Secondly, focusing transducer could be used [15] to direct the beam onto the rings. However this requires a liquid coupling medium through which to focus the wave. Thirdly, high frequency piezoelectric films could be used. This involves the deposition of a thin layer of piezoelectric aluminum nitride film onto the surface. This is then achieved over small region. This approach was used successfully to measure the oil film in a rolling element bearing [16].

Once the reflection coefficient was obtained, the lubricant film thickness could be calculated by employing the spring model equation (6). The speed of sound in and density of this oil are 1400 m/s and 880 kg/m³ respectively and the acoustic impedance of the piston ring is 34.44 MRayls. Figure 11 shows the oil film thicknesses for the piston ring-wall contact with an engine speed of 840 rpm.

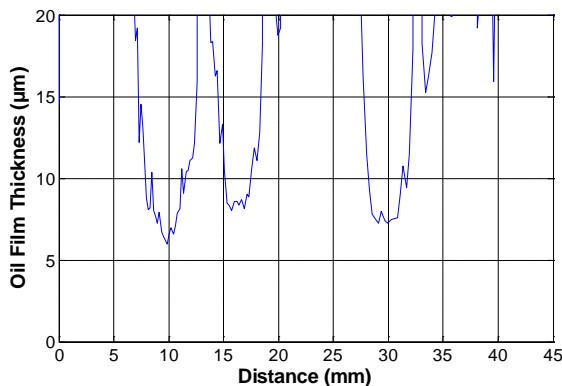


Figure 11. Plot of measured oil film thickness for an engine speed of 840 rpm.

If the minimum reflection coefficients given in Figure 9 are used, minimum oil film thickness is obtained. However, at this stage, Figure 12, showing “approximate” minimum oil film thickness, is just given as an indication due to the spatial resolution problem mentioned above.

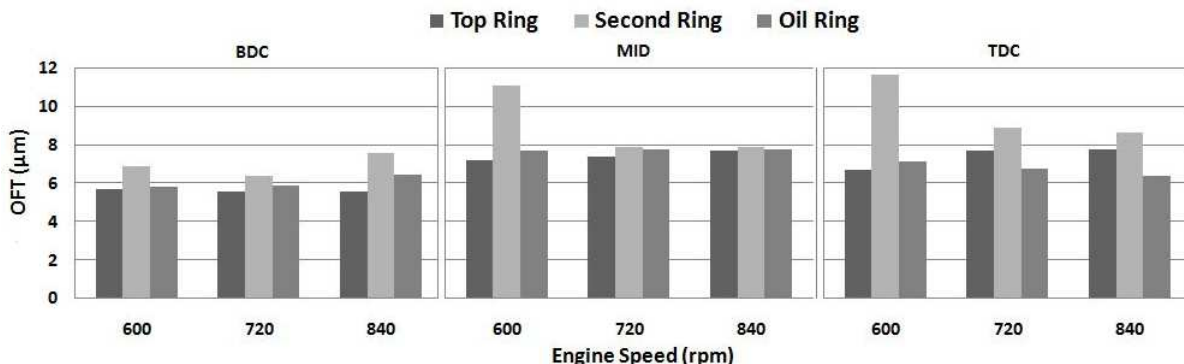


Figure 12. “Approximate” minimum oil film thickness in the rings for engine speeds of 600,720 and 840 rpm.

The range of OFT values, varying from 5 to 10 µm, approximately matched those from the literature, especially for motored engine studies (see Table 1). Dhar [4] measured piston ring film thickness in motored engine using a capacitance probe and the results were ranging from 0.2 to 8 µm. Another study using LIF method was carried out by Baba [9]. The results showed that oil film thickness for piston ring was varying from 5 to 18 µm.

As shown in Figure 12, the measurements at close BDC had the smallest group of oil film thickness for the rings, ranging from 5.5 µm to 7.5 µm. The OFT values were increased for MID location where the velocity of piston was greatest. This is expected from hydrodynamic theory, the higher entrainment speed the higher the film thickness however the speed effect on OFT values is not

strong. At close to TDC where entrainment speed was lower than of the MID location, there were some anomalies occurring in the second ring OFT values such that OFT was greatest at 600 rpm. The identification of these anomalies is difficult with this test rig because only piston speed can be controlled. The oil film pressure supports only the pressure produced by the inherent ring radial force. The circumferential conformability could be different from BDC to TDC, this could also have an effect on piston ring oil film thickness values. There is no cooling system on the test rig and therefore the higher speeds lead to higher oil temperature. This reduced viscosity and the load carrying capacity of oil film and so the film thickness is decreased to stabilize the pressure load.

Density of the oil assumed to be constant for the OFT calculation; however temperature at near measurement area was increased from 15 °C to 40 °C during the tests period. A change of the oil density due to this temperature increment was about 1.82 % so given the linear dependence on density, an equivalent error would be present in the OFT values (roughly a difference of 0.12 μm). Also a standard deviation of measured R values was 0.0039. If the measured reflection coefficient range (from 0.88 to 0.97) has been considered, the estimated error in the OFT values would be between 1.9% for 0.88 of R and 7.5% for 0.97 of R according to the equation (6).

CONCLUSION

Several measurements were taken from near TDC, BDC and at mid stroke of a motored engine. The transducer has successfully detected the ring pack and the reflection coefficient has been generated for different engine speeds. Oil film thickness values can be obtained from spring model using the reflection coefficient data if the incident ultrasound can be confined to fall entirely on the ring surface. The obtained minimum OFT values for the rings were rough due to the spatial resolution problem. Several ideas for the application of the ultrasound technique to piston ring have been given to solve the resolution problem. The use of higher capacity internal memory and a more powerful ultrasonic signal would increase the system sensitivity. This study has shown that non-invasive oil film thickness measurements between the piston ring and liner is feasible using the ultrasonic approach.

REFERENCES

1. Furuhashi, S., Asahi, C., and Hiruma, M., "Measurement of Piston Ring Oil Film Thickness in an Operating Engine," ASLE Transactions **26** (3):325-332, 1982.
2. Söchtig, S. J., and Sherrington, I., "The Effect of Load and Viscosity on the Minimum Operating Oil Film Thickness of Piston-Rings in Internal Combustion Engines," Proc. IMechE, Part J: J. Engineering Tribology **223**:383-391, 2009.
3. Sherrington, I., and Smith, E. H., "Experimental Methods for Measuring the Oil-film Thickness between the Piston-rings and Cylinder-wall of Internal Combustion Engines," Tribology International **18**,(6): 315-320, 1985.
4. Dhar, A., Agarwal, A. K., and Saxena, V., "Measurement of Dynamic Lubricating Oil Film Thickness between Piston Ring and Liner in a Motored Engine," Sensors and Actuators A: Physical **149**:7-15, 2009.
5. Richardson, D. E., and Borman, G. L., "Using Fibre Optics and Laser Fluorescence for Measuring Thin Oil Films with Applications to Engines," SAE Technical Paper 912388, 1991.
6. Seki, T., Nakayama, K., Yamada, T., Yoshida, A., and Takiguchi, M., "A Study on Variation In Oil Film Thickness of a Piston Ring Package: Variation of oil film thickness in piston sliding direction," JSAE Review **21**:315-320, 2000.
7. Taylor, R. I., and Evans, P. G., "In-Situ Piston Measurements," Proceedings of the IMech.E, Part J. **218**:185-200, 2004.
8. Takiguchi, M., Nakayama, K., Furuhashi, S., and Yoshida, H., "Variation of Piston Ring Oil Film Thickness in an Internal Combustion Engine - Comparison Between Thrust and Anti-Thrust Sides," SAE Technical Paper 980563, 1998.
9. Baba, Y., Suzuki, H., Sakai, Y., Wei, D. L. T., Ishima, T., and Obokata, T., "PIV/LIF Measurements of Oil Film Behavior on the Piston in I. C. Engine," SAE Technical Paper 2007-24-0001, 2007.
10. Tamminen, J., Sandström, C. E., and Andersson, P., "Influence of Load on the Tribological Conditions in Piston Ring and Cylinder Liner Contacts in a Medium-Speed Diesel Engine," Tribology International **39**:1643-1652, 2006.
11. Tattersall, H. G., "The Ultrasonic Pulse-Echo Technique as Applied to Adhesion Testing," J. Appl. Phys. **6**:819-832, 1973.

12. Dwyer-Joyce, R. S., Green, D. A., Harper, P., Lewis, R., Balakrishnan, S., King, P. D., Rahnejat, H., and Howell-Smith, S., "The Measurement of Liner-Piston Skirt Oil Film Thickness by an Ultrasonic Means," SAE Technical Paper 2006-01-0648, 2006.
13. Dwyer-Joyce, R. S., Drinkwater, B. W., and Donohoe, C. J., "The Measurement of Lubricant-Film Thickness Using Ultrasound," Proc. Royal Society, **459**:957-958, 2003.
14. Dwyer-Joyce, R. S., Harper, P., and Drinkwater, B., "Oil Film Measurement in Polytetrafluoroethylene-Faced Thrust Pad Bearings for Hydrogenerator Applications," Proc. IMechE Part A: Journal of Power and Energy **220**:619-628, 2006.
15. Dwyer-Joyce, R. S., Reddyhoff, T., and Drinkwater, B., "Operating Limits for Acoustic Measurement of Rolling Bearing Oil Films Using Ultrasonic Reflection," Tribology Transactions **47**:366-375, 2004.
16. Dwyer-Joyce, R. S., Drinkwater, B. W., Zhang, J., Elgoyhen, J., Kirk, K. J., "Instrumentation of a Rolling Bearing with a Thin Film Piezo Coating for Oil Film Measurement," Proceedings of the ASME/STLE International Joint Tribology Conference (IJTC) 2007, vol part A, 383-385, 2008.

CONTACT INFORMATION

Emin Yusuf AVAN

The Leonardo Centre for Tribology
The University of Sheffield
Sir Frederick Mappin Building
Mappin Street
Sheffield
UK
S1 3JD
Tel: +44 (0)1142 227771
E-mail: e.y.avan@sheffield.ac.uk